Rigorous Calculations and Measurements of $A_y(\theta)$ for $n+d$ Elastic-Scattering and Breakup Processes

C. R. Howell, W. Tornow, I. Slaus, P. D. Felsher, M. L. Roberts, H. G. Pfützner, Anli Li, K. Murphy, and R. L. Walter
Department of Physics, Duke University, and Triangle Universities Nuclear Laboratory, Durham, North Carolina 27706

J. M. Lambert and P. A. Treado
Department of Physics, Georgetown University, Washington, D.C. 20007

and

H. Witała, W. Glöckle, and T. Cornelius
Institut für Theoretische Physik, Ruhr-Universität Bochum, D-4630 Bochum, Federal Republic of Germany
(Received 18 April 1988)

The vector analyzing power for the $n+d \rightarrow n+n+p$ breakup reaction was measured at 12 MeV. Data for n-p final-state interaction and n-p quasifree scattering, along with elastic-scattering data, are compared to rigorous three-nucleon calculations using the Paris and Bonn N-N potentials. Calculations agree with the quasifree data and with the elastic and n-p final-state-interaction data except around $\theta_{\text{c.m.}} = 120°$.

PACS numbers: 25.10.+s, 24.70.+s, 25.40.Dn, 25.40.Fq

Recently, considerable progress has been achieved both in the calculation of the three-nucleon ($3N$) scattering observables[1] and in the accuracy of neutron-deuteron (n-d) elastic-scattering data.[2] Such $3N$ scattering calculations are now done with use of nucleon-nucleon (N-N) potentials based on realistic meson-exchange theory, e.g., Paris[3] and Bonn[4] potentials, and the Faddeev equations[5] are solved rigorously. In previous works by other groups various approximations were made. For elastic scattering, separable finite-rank approximations to the Paris and Bonn potentials[2,6] and phenomenological N-N potentials[7] were used, while for the breakup process, calculations were performed with phenomenological separable[8] and local (treating higher partial waves perturbatively)[9] potentials. We are now able to solve the three-nucleon continuum problem rigorously (i.e., with high numerical accuracy[10]) using N-N forces based on meson-exchange theory. Only for this case can one be sure that discrepancies with experimental data indicate a defect of the input nuclear interaction. Our calculations are restricted to n-d scattering, thus avoiding the still pending Coulomb problem. The comparison between $3N$ calculations and n-d data is essential, since some three-body observables, e.g., analyzing powers, display more sensitivity to certain N-N partial-wave interactions than the two-body observables. Furthermore, $3N$ force effects can be determined only from studies of the $3N$ system. In the present Letter we report n-d predictions for the vector analyzing power $A_y(\theta)$ using the Paris potential[3] and the Bonn relativistic one-boson-exchange potential in q space (OBEPQ)[4] and compare them with our elastic-scattering and breakup data obtained at an incident neutron energy of 12 MeV. These data are the highest-accuracy data for these observables.

While n-d breakup cross sections have been measured extensively,[11] the $A_y(\theta)$ have been measured only for the neutron-proton (n-p) final-state interaction (FSI) at 14.3 and 29.6 MeV (Ref. 12) with monoenergetic neutron beams and at nine energies from 20 to 50 MeV with use of a continuous-energy neutron beam.[13] Kinematically complete measurements of cross section and $A_y(\theta)$ for $n+d$ breakup reactions are in progress by Geissdörfer *et al.* at 13.9 MeV.[14]

The experimental study of the ${}^2\mathrm{H}(n,np)n$ reaction was conducted at the Triangle Universities Nuclear Laboratory with polarized neutrons bombarding a deuterated scatterer (C_6D_{12}) in the form of a liquid scintillator, which allowed a measurement of the energy of the outgoing proton. The polarized neutrons were produced via the ${}^2\mathrm{H}(\vec{d},\vec{n})^3\mathrm{He}$ source reaction induced by polarized deuterons. The neutron-beam polarization was determined from the measured deuteron-beam polarization and the polarization transfer coefficients[15] for the reaction ${}^2\mathrm{H}(\vec{d},\vec{n})^3\mathrm{He}$. Typically, the incident-deuteron-beam polarization was 62%, thereby producing a neutron-beam polarization of 55%. The scattered neutrons were detected by two pairs of shielded scintillators and their energies were determined by the time of flight from the deuterated scintillator to each side detector. A valid event required a coincidence between events in the deuterated scintillator and in a side detector. For each event we measured the energy of the outgoing proton and the energy and direction of the scattered neutron. Such an event is underdetermined by one kinematic variable, e.g., the direction of the proton. We denote a scattered neutron by 1, a proton by 2, and the undetected neutron by 3. Along the kinematic boundary, the polar angle θ and azimuthal angle ϕ of the proton have unique values; thus all events along the boundary are fully determined kinematically. For each neutron-scattering angle the region adjacent to the largest allowed E_{n1} is the p_2-n_3 FSI, and the two n_1-p_2 quasifree-scattering (QFS) conditions are on the boundary.

In our measurement the incident neutron energy spread, finite geometry, and detector energy resolution give an overall energy resolution for n_1 and p_2 of 0.4 MeV. The overall angular resolution due to finite geometry and finite energy intervals for n_1 and p_2 used in the analysis of the data depends on the neutron angle; for the p_2-n_3 FSI it is largest ($\Delta\theta_{\text{c.m.}}=3°$) at $\theta_{\text{c.m.}}=130°$; for n_1-p_2 QFS $\Delta\theta_{\text{c.m.}}$ increases from 1° at $\theta_{\text{c.m}}=20°$ to 10° at $\theta_{\text{c.m.}}=100°$. The threshold for charged-particle detection in the deuterated scintillator was 0.1 MeV, while that of the neutron side detectors was 0.6 MeV.

We have measured elastic-scattering (published already[2]) and breakup processes at fourteen laboratory neutron angles between $\theta_{n1}=16°$ and 115°. This gave cross-section and $A_y(\theta)$ data for n_1-p_2 QFS and the p_2-n_3 FSI, as well as data on the collinear configuration (one nucleon is at rest in the overall c.m. system), the star configuration (the three c.m. momenta have equal magnitude and point to the vertices of an equilateral triangle), and the n_1-n_3 and n_1-p_2 FSI configurations. This measurement, as opposed to that of Ref. 14, covers almost the entire $3N$ phase space. In this paper we report $A_y(\theta)$ for the p_2-n_3 FSI and n_1-p_2 QFS.

The measured $n+d$ breakup data were corrected[16] for accidental coincidence events and multiple-scattering and finite-geometry effects. Typically, accidental and multiple-scattering events amounted to about 7% of the experimental yield in the p_2-n_3 FSI and n_1-p_2 QFS regions. The corrections to $A_y(\theta)$ due to accidental background and to multiple scattering are typically 0.01 each. The uncertainties in $A_y(\theta)$ from these corrections are less than 0.002. A systematic error due to the uncertainty in the polarization transfer coefficient for the $^2\text{H}(\vec{d},\vec{n})^3\text{He}$ reaction and in the polarization of the deuteron beam is less than 3%; this error enters as a scale factor of 1.00 ± 0.03. Since $A_y(\theta)<0.2$, the absolute error due to this scale uncertainty is less than 0.006. Numerical errors in our $3N$ calculations are smaller[10] than the total experimental uncertainty.

We solved Faddeev equations in the form $T=tP+tG_0PT$. Here G_0 is the free propagator, P is the sum of two cyclical permutations of three objects, and t is the two-body t operator. The operator T determines the transition operators for elastic n-d scattering and the breakup process.[1] These equations are solved in momentum space and in a partial-wave basis. We use the Paris potential and the Bonn OBEPQ. For both potentials, the two nucleons were allowed to act in the $^1S_0$, $^3S_1$-$^3D_1$, $^3P_0$, $^1P_1$, $^3P_1$, $^3P_2$-$^3F_2$, $^1D_2$, and $^3D_2$ states, i.e., in all N-N angular momentum states with $J\leq 2$. The observables were calculated for kinematically complete configurations and then an integration was performed over the unobserved angles θ and ϕ of the proton. Since our experimental data are averages over finite E_{n1}-E_{p2} intervals, the theoretical values were averaged over the corresponding intervals.

The comparison between theory and experiment (circles) for the n_1-p_2 QFS data for $A_y(\theta)$ is presented in Fig. 1. The width of the averaging intervals (ΔE_n and ΔE_p) for the experimental QFS data varied from 1 to 2 MeV as θ_n varied. Over this energy interval the spectator energy is below 0.5 MeV. The crosses and asterisks in Fig. 1 represent predictions for the Paris and OBEP potentials, respectively, averaged over the energy intervals of the experiment. The theoretical results averaged over the smaller interval of 800 keV are slightly more negative (solid and dashed curves). The dotted curves are the $A_y(\theta)$ for free n-p scattering at 12 MeV (top curve) and 7.52 MeV calculated with use of the Paris potential.

Both measured and predicted $A_y(\theta)$ for QFS are small, about -0.02. Agreement between the data and predictions is quite good. The difference between the predictions of the Paris and OBEPQ potentials is negligible, typically 0.001. The $A_y(\theta)$ for QFS differs in sign from that for n-p free scattering. This difference implies that the contributions from higher-order terms in the three-body scattering are very large at these energies. [Further evidence of the importance of these terms is that $A_y(\theta)$ calculated using the impulse approximation is positive and lies roughly between the two dotted curves.]

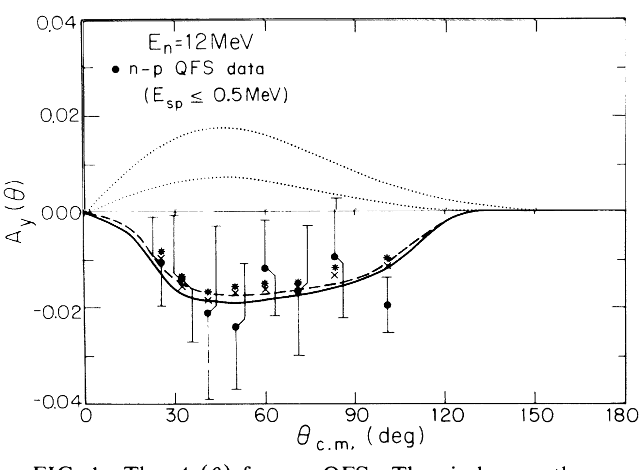

FIG. 1. The $A_y(\theta)$ for n-p QFS. The circles are the measurements. The crosses and asterisks represent the Paris- and Bonn-potential predictions integrated over energy intervals used in the data analysis. The solid and dashed curves are Paris- and Bonn-potential predictions, respectively, integrated over an 800-keV energy interval. The dotted curves are the Paris predictions for free n-p scattering at $E_n(\text{lab})=7.52$ and 12 MeV (top curve).

Although the OBEPQ differs from the Paris potential in the ${}^3S_1$-${}^3D_1$ force, that force component has a negligible influence on the analyzing power in free *n-p* scattering. According to our calculation the multiple-scattering processes do not enhance the ${}^3S_1$-${}^3D_1$ influence; the difference in the A_y predictions for Paris and OBEPQ potentials comes mainly from the ${}^3P_J$ force component.

The $A_y(\theta)$ for *n-d* elastic scattering and for p_2-n_3 FSI corresponding to $E_{p_2n_3} \leq 1.0$ MeV are shown at the top of Fig. 2. The curves are the predictions of the Paris and OBEPQ potentials. In the lower part of Fig. 2 we show the sensitivity of the predictions of the Paris potential for the different $E_{p_2n_3}$ relative-energy intervals of 0–0.5, 0–1, and 1–2 MeV. The maximum in $A_y(\theta)$ systematically moves to smaller $\theta_{\text{c.m.}}$ as $E_{p_2n_3}$ increases, shifting from 135° for FSI($E_{p_2n_3}$=0–0.5 MeV) to 120° for FSI($E_{p_2n_3}$=1–2 MeV). These positions can be compared to that for the maximum for elastic scattering which occurs at 125°. The measured $A_y(\theta)$ for $E_{p_2n_3}$=1–2 MeV, which are also graphed in the lower part of Fig. 2, compare reasonably well with the corresponding 1–2-MeV prediction (dot-dashed curve).

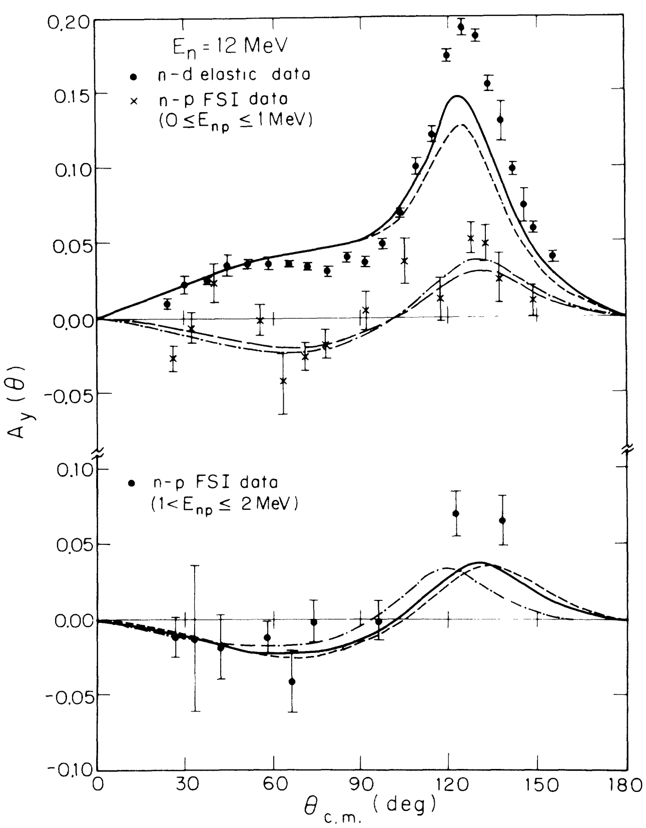

FIG. 2. Top: $A_y(\theta)$ data for the *n-p* FSI in the ${}^2\text{H}(\vec{n},n_1p_2)n_3$ reaction corresponding to $E_{p_2n_3} \leq 1.0$ MeV (crosses) and for *n-d* elastic scattering (circles) together with three-body calculations using the Paris (solid and dot-dashed curves) and Bonn (short-dashed and long-dashed curves) potentials. Bottom: calculations with Paris potential for the *n-p* FSI with $E_{p_2n_3}$=0–0.5 MeV (dashed curve), 0–1 MeV (solid curve), and 1–2 MeV (dot-dashed curve), together with data for $E_{p_2n_3}$=1–2 MeV (circles).

At forward angles the $A_y(\theta)$ for elastic scattering are influenced by ${}^1S_0$, ${}^3S_1$-${}^3D_1$, and ${}^3P_J$ forces. Although these forces differ for the Paris and OBEPQ potentials, the final predictions for the potentials are the same at forward angles for elastic scattering and quite similar for inelastic scattering. However, the difference between $A_y(\theta)$ for elastic and inelastic processes, experimental as well as calculated, is very pronounced at forward angles: The contribution of the ${}^1S_0$ wave to the *n-p* FSI $A_y(\theta)$ is large and negative and it overrides the positive contribution of the ${}^3S_1$-${}^3D_1$. This together with the fact that the ${}^1S_0$ contribution increases with decreasing $E_{p_2n_3}$ causes the maximum of $A_y(\theta)$ to shift to larger angles for smaller $E_{p_2n_3}$. Our three-body calculation agrees well with both elastic and inelastic $A_y(\theta)$ data at forward angles. However, there are pronounced discrepancies near $\theta_{\text{c.m.}}$=120°. These are appreciable for elastic scattering and are also present in both FSI angular distributions. Our rigorous calculation confirms the discrepancy seen in the earlier study[2] of the elastic scattering using finite-rank approximation to the Paris potential; in the present calculation the discrepancy is even larger. Inclusion of the *N-N* force for $J=3$ increases this discrepancy.[10] Elastic scattering at backward angles is dominated by ${}^3P_J$ forces and the effect of the ${}^3S_1$-${}^3D_1$ force is rather small. Differences between Paris and OBEPQ predictions (see Fig. 2) are due to their different ${}^3P_J$ phases and $A_y(120°)$ is a magnifying glass for the ${}^3P_J$ forces. The breakup processes give additional information about the *N-N* force to those provided by elastic scattering[17]; for example, Fig. 2 clearly shows the role played by the ${}^1S_0$ force.

The discrepancies around 120° could be reduced by modifying ${}^3P_J$ phases, and in fact neither Paris nor OBEPQ reproduce all *N-N* phases and observables sufficiently well.[18] However, it is not clear whether these discrepancies can be cured by modifying ${}^3P_J$ phases when a fit to data for *n-p* and *p-p* free scattering is also required, even if charge-symmetry breaking is allowed not only in ${}^1S_0$ but also in ${}^3P_J$ states. It is important that the nuclear dynamics is transported rigorously into theoretical observables and is not obscured by approximations. While this stage was achieved for the 3*N* bound states a few years ago, it has only now been achieved for the 3*N* continuum. This opens the door to testing of *N-N* and 3*N* forces, and the *n-d* interaction provides a rich ground for such studies.[19]

We acknowledge the assistance of A. A. Naqvi, M. Al Ohali, and G. Mertens and support of the U.S. Department of Energy, Office of High Energy and Nuclear Physics, under Contract No. DE-AC05-76ER01067, the U.S.–Yugoslav Joint Board Contract No. JF 682, and the Deutsche Forschungsgemeinschaft under Contract No. To69/7.

[1]H. Witała, W. Glöckle, and T. Cornelius, Few Body Syst., Suppl. **2**, 555 (1987).

[2]C. R. Howell *et al.*, Few Body Syst. **2**, 19 (1987).

[3]M. Lacombe *et al.*, Phys. Rev. C **21**, 861 (1980).

[4]R. Machleidt, K. Holinde, and Ch. Elster, Phys. Rep. **149**, 1 (1987).

[5]L. D. Faddeev, Zh. Eksp. Teor. Fiz. **39**, 1459 (1960) [Sov. Phys. JETP **12**, 1014 (1961)].

[6]Y. Koike, J. Haidenbauer, and W. Plessas, Phys. Rev. C **35**, 396 (1987); W. Plessas and J. Haidenbauer, Few Body Syst., Suppl. **2**, 185 (1987).

[7]J. J. Benayoun *et al.*, Phys. Rev. Lett. **36**, 1438 (1976); T. Takemiya, Prog. Theor. Phys. **74**, 301 (1985).

[8]P. Doleschall, Phys. Lett. **38B**, 298 (1972); J. Bruinsma and R. van Wageningen, Nucl. Phys. **A282**, 1 (1977); P. Doleschall *et al.*, Nucl. Phys. **A380**, 72 (1982).

[9]C. Stolk and J. A. Tjon, Nucl. Phys. **A319**, 1 (1979).

[10]H. Witała *et al.*, to be published, and Few Body Syst. **3**, 123 (1988).

[11]See D. R. Tilley *et al.*, Nucl. Phys. **A474**, 1 (1987).

[12]R. Fischer *et al.*, in *Few Body Systems and Nuclear Forces I,* edited by H. Zingl, M. Haftel, and H. Zankel, Lecture Notes in Physics Vol. 82 (Springer-Verlag, Berlin, 1978), Vol. 1, p. 259.

[13]H. O. Klages *et al.*, in *The Three-Body Force in the Three-Nucleon System,* edited by B. L. Berman and B. F. Gibson, Lecture Notes in Physics Vol. 260 (Springer-Verlag, Berlin, 1986), p. 311; H. O. Klages, *ibid.*, p. 203.

[14]K. Geissdörfer *et al.*, Verh. Dtsch. Phys. Ges. **23**, 104 (1988).

[15]P. W. Lisowksi *et al.*, Nucl. Phys. **A242**, 298 (1975).

[16]C. R. Howell *et al.*, in Triangle Universities Nuclear Laboratory Annual Reports No. XXIII, 1984 (unpublished), p. 21, and No. XXV, 1986 (unpublished), p. 28; C. R. Howell *et al.*, in Ref. 13, p. 229.

[17]Y. Koike and Y. Taniguchi, Few Body Syst. **1**, 13 (1984).

[18]W. Tornow *et al.*, Phys. Rev. C **37**, 2326 (1988); J. Sromicki *et al.*, Phys. Rev. Lett. **57**, 2359 (1986); J. J. deSwart, Nucl. Phys. **A416**, 299c (1984).

[19]I. Šlaus *et al.*, Phys. Rev. Lett. **48**, 993 (1982); W. Meier and W. Glöckle, Phys. Lett. **138B**, 329 (1984); B. F. Gibson and B. H. J. McKellar, Few Body Syst. **3**, 143 (1988).